THICK-FILM RESISTORS WITH LOW AND HIGH TCRS ON LTCC SUBSTRATES

Marko Hrovat[1], Darko Belavič[2], Jaroslaw Kita[3], Janez Holc[1], Jena Cilenšek[1], Leszek Golonka[3], Andrzej Dziedzic[3]

[1]Jožef Stefan Institute, Ljubljana, Slovenia
[2]HIPOT-R&D, d.o.o., Šentjernej, Slovenia
[3]Wroclaw University of Technology, Wroclaw, Poland

Key words: thick-film, resistors, NTC, LTCC, interactions, electrical parameters

Abstract: Low-Temperature Co-fired Ceramic (LTCC) materials, which are sintered at the low temperatures typically used for thick-film processing, i.e., around 850°C, are widely used for ceramic multi-chip modules (MCM-C). Thick-film resistors with low TCRs (Du Pont, 2041, nominal sheet resistivity 10 kohm/sq.) and thick-film NTC thermistors with high negative TCRs (EMCA-Remex, 4993, nominal resistivity 1 kohm/sq.) which were developed for alumina substrates, were evaluated on glassy LTCC substrates. The electrical and microstrutural characteristics of films fired on alumina or co-fired on "green" LTCC substrates were compared. The electrical characteristics (TCRs, sheet resistivities and noise indices) of 2041 resistors fired on both substrates are similar indicating that the resistors are compatible with the LTCC material. In the case of the NTC 4993 thermistors the resistivities, beta factors and noise indices of the thermistors fired on LTCC substrates significantly increased, indicating the interactions between the thermistor layers and the LTCC substrates. The changes in the electrical parameters were attributed to the diffusion of a silica-rich phase from the LTCC into the thermistor films.

Debeloplastni upori z nizkimi in visokimi odvisnostmi upornosti od temperature na LTCC substratih

Kjučne besede: debeli filmi, upori, NTC, LTCC, interakcije, električne karakteristike

Izvleček: Keramika z nizko temperature žganja (LTCC - Low temperature co-fired ceramics) se sintra pri temperaturah, tipičnih za debeloplastno tehnologijo, to je okrog 850°C. Uporablja se za izdelavo keramičnih večplastnih struktur (MCM-C). Debeloplastni upori z nizkimi TCR (Du Pont, 2041) in debeloplastni NTC termistorji (EMCA Remex, 4993), ki so bili razviti za žganje na inertnih Al_2O_3 substratih, so bili testirani na steklastih LTCC podlagah. Primerjane so električne in mikrostrukturne karakteristike plasti, žganih na Al_2O_3 in LTCC podlagah. Električne karakteristike (plastne upornosti, TCR in šum) 2041 uporov, žganih na obeh vrstah podlag, so primerljivi, kar pomeni, da so testirani upori kompatibilni z reaktivnimi LTCC podlagami. Za NTC 4993 termistorje so rezultati pokazali, da upornosti, beta faktorji (strmina odvisnosti upornosti od temperature) in šum narastejo po žganju na LTCC podlagah. Spremembe električnih karakteristik pripisujemo predvsem difuziji SiO_2 bogate steklaste faze med žganjem iz LTCC v NTC upore.

Introduction

Ceramic multi-chip modules (MCM-Cs) are multilayer substrates with buried conductor lines, which means they have a high density of interconnections. An additional advantage of the smaller size and higher density is the ability to integrate screen-printed resistors, or occasionally, capacitors and inductors. These screen-printed components can be placed either beneath the discrete components on the surface of the multilayer dielectric or buried within the multilayer structure. Low-temperature co-fired ceramic (LTCC) materials, which are sintered at the low temperatures typically used for thick-film processing, i.e., around 850°C, are widely used for the production of MCM-Cs, especially for telecommunications and automotive applications. LTCCs are either based on crystallisable glass or a mixture of glass and ceramics; for example, alumina, silica or cordierite ($Mg_2Al_4Si_5O_{18}$) /1-6/. The composition of the inorganic phase in most LTCC tapes is similar to, or the same as, materials in thick-film multilayer dielectric pastes. To sinter to a dense and non-porous structure at these, rather low, temperatures, it has to contain some low-melting-point glass phase. This glass would (or could) presumably interact with, for example, thick-film resistors leading to changes in the electrical characteristics. Some of the results for the resistor/LTCC combinations and the influences on the electrical characteristics can be found in /7-10/.

The main required characteristics for thick-film resistor materials are a long-term stability and relatively narrow tolerances of the sheet resistivities after firing. A very important characteristic is a low temperature coefficient of resistivity (TCR), which for most modern resistors is around or under $100x10^{-6}$/K. However, for temperature-sensing or temperature compensating applications the resistors with a large temperature dependence of resistivity - thermistors -are required. The thermistors with negative TCRs have very large and strongly non-linear temperature vs. resistivity dependence. The dependence of the specific resistance ρvs. temperature is described by:

$$\rho = \rho_0 \times \exp(B/T) \quad (1)$$

where ρ_0 is the resistivity (ohm.cm) at "infinite" temperature, T(K) is the temperature and B (K) is the thermistor constant (also called the beta factor or the coefficient of temperature sensitivity). Resistivity at "infinite" temperature is determined by the total number of "B" lattice sites in a spinel structure that can take part in the "hopping" conductivity process (there is no contribution to the overall conductivity if ions with different valences are on the A sites because the distance between the two A sites in a spinel lattice is too great for an electron "hopping" mechanism). The B is defined as the ratio between the activation energy for electrical conduction and the Boltzman constant. Basically it is a "steepness" of the resistivity vs. temperature curve. For the calculation of B from measured resistances at different temperatures the equation (1) is normally rewritten as

$$B = \ln (R_1/R_2) / (1/T_1 - 1/T_2) \quad (2)$$

where T(K) is again the temperature and R_1 and R_2 (ohm) are the resistances at T_1 and T_2, respectively.

These materials with large, negative TCRs (NTC) are based on solid solutions of transition-metal oxides. Mostly, due to their long-term stability, the compounds are solid solutions of Mn_3O_4, Co_3O_4 and NiO oxides with the spinel structure /11-13/. The general formula of the spinel structure is AB_2O_4. It is based on oxygen atoms arranged in an fcc (face-centred-cubic) structure containing tetrahedral (A) and octahedral (B) lattice sites. The electrical charge transport is via the hopping of electrons between the B^{3+} and B^{4+} ions present at the octahedral sites in the lattice. This is shown schematically in Fig. 1 for the NiO-doped Mn_3O_4. The spinel Mn_3O_4 (Mn^{2+} $2Mn^{3+}O_4$) is non-conducting. When some of the manganese 3+ ions are substituted by the nickel 2+ ions the same number of manganese ions change their valence from 3+ to 4+ in order to preserve the overall electrical neutrality. Electron hopping between the Mn^{3+} and the Mn^{4+} can take place.

The values of the resistivities and the beta factors of the NTC materials depend on the ratio of the oxides. The resistivities range from a few hundred ohm.cm to a few tens of kohm.cm, and the beta factors from 2500 K to 4000 K. These electrical characteristics are shown in the ternary phase diagram of Mn-Co-Ni-oxides for the resistivities (Fig. 2.a) and the beta factors (Fig. 2.b) /13/. The compositions with minimum resistivities, and maximum and minimum beta factors are indicated by arrows. The solid solutions with the lowest resistivities (rich on manganese oxide) also have the lowest temperature coefficients of expansion, i.e. 8.2×10^{-6}/K. A partial substitution of the iron ions (3+) on the B sites or the copper ions (1+) on the A sites increases or decreases the resitivities, respectively /14-17/.

Conductivity – electron "hopping"

"A" sites	"B" sites		
Mn^{2+}	$Mn^{3+}Mn^{3+}$	O_4	– non-conducting
	$\mathbf{xNi^{2+}}$ $\mathbf{xMn^{4+}}(2\text{-}x)Mn^{3+}$	O_4	- conducting

$Mn^{4+} + e^- \text{----------} > Mn^{3+}$

Fig. 1. Conductivity mechanism in NiO-doped Mn_3O_4 spinel - schematic

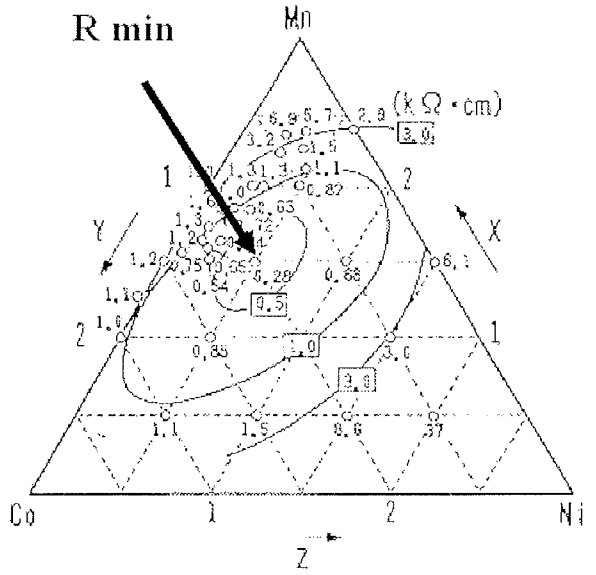

Fig. 2.a: Ternary phase diagram of Mn-Co-Ni-oxides. The minimum resistivity is indicated by the arrow /13/

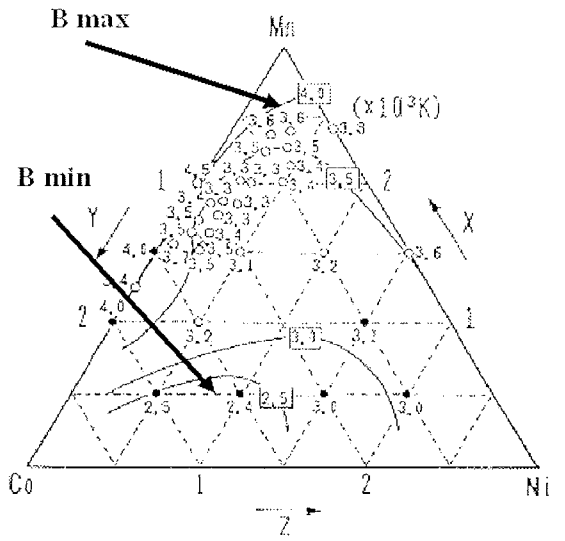

Fig. 2.b: Ternary phase diagram of Mn-Co-Ni-oxides. The maximum and minimum beta factors are indicated by the arrows /13/

The fired thickness of the thick-film layers is usually between ten and twenty micrometers. As mentioned before, the resistivities of the different spinel compositions are between a few hundred ohm.cm and a few tens of kohm.cm, and can be increased up to 1 Mohm.cm with the partial substitution of manganese ions with iron ions. These are useful values for pellet-type components. How-

ever, due to the dimensions of the thick-film resistors the values of the sheet resistivities (ohm/sq.) are between two and three orders of magnitude higher than the resistivities (ohm.cm) of the materials themselves. The glass phase, which is added for better sintering of the thick-film layers at relatively low firing temperatures (850°C), further increases the resistivity. Therefore, materials for thick-film NTC resistors usually include some phase with a low specific resistance, generally RuO_2. RuO_2 has a relatively low specific resistivity, 40 x 10^{-6}ohm.cm, and a positive, linear, metallic-like dependence of resistivity vs. temperature, with a TCR of 7000x10^{-6}/K for single crystals and a few 1000x10^{-6}/K for sintered microcrystalline samples /18,19/. The addition of ruthenium oxide decreases the specific resistance, reduces the noise and improves the stability of the resistors. However, due to the RuO_2 high, positive and linear metallic-like TCR /14,20/ it also decreases the beta factors.

As most of the thick-film resistors were developed for firing on alumina substrates their compatibility with (rather glassy) LTCC substrates needs to be evaluated. The aim of this work is to compare the electrical and microstrutural characteristics of the low TCR "normal" thick-film resistor 2041 (10 kohm/sq., Du Pont) and the 4993 NTC thermistor (1 kohm/sq., EMCA Remex) fired on 96% alumina and co-fired on Du Pont LTCC 951 substrates. The 2041 resistor was chosen because of its high stability and low noise. The conductive phase is based on a mixture of RuO_2 and $Pb_2Ru_2O_{6.5}$ /21,22/. The nominal beta factor of NTC 4993 thermistors is 1200 K. As mentioned above, both thick-film materials were developed for alumina substrates.

The X-ray spectra of the Du Pont LTCC 951 tapes, unfired and fired at 850°C, are shown in Fig. 3 /23/. The unfired material is a mixture of alumina and glass. After firing, peaks of anorthite ($(Na,Ca)(Al,Si)_4O_8$) phase appear. The peaks of alumina and anorthite are denoted by "A" and asterisk, respectively.

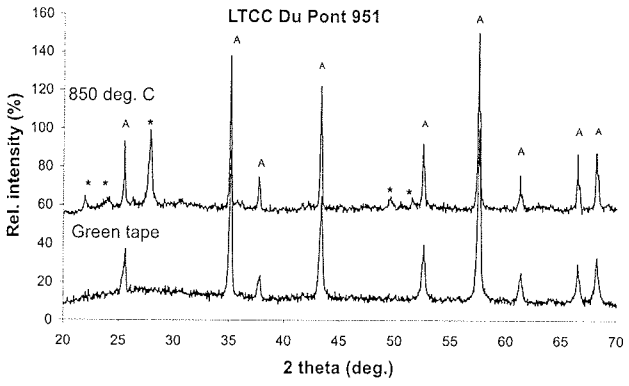

Fig. 3: X-ray spectra of green and fired (850°C) Du Pont LTCC 951 tapes /16/. The peaks of alumina and anorthite are denoted "A" and asterisk, respectively

Experimental

The 2041 resistors and NTC 4993 thermistors were screen printed and fired for 10 min at 850°C on 96% alumina and on green LTCC (951, Du Pont) substrates. The LTCC substrates were made by laminating three layers of LTCC tape at 70°C and at a pressure of 200 bar. The thick-film resistors were terminated by Pd/Ag electrodes that were pre-fired at 850°C on alumina substrates, and cofired together with the printed thermistors and LTCC substrates. The dimensions of the resistors for the microstructural analysis and the X-ray diffraction (XRD) analysis, which were printed and fired without conductor terminations, were 12.5x12.5 mm^2.

For the microstructural investigation the samples were mounted in epoxy in a cross-sectional orientation and then cut and polished using standard metallographic techniques. A JEOL JSM 5800 scanning electron microscope (SEM) equipped with an energy-dispersive X-ray analyser (EDS) was used for the overall microstructural and compositional analysis. Note that boron oxide, which is also present in the glass phase, cannot be detected in the EDS spectra because of the low relative boron weight fraction in the glass and the strong absorption of the boron K_α line during EDS analysis in the glass matrix. Dried thermistors (150°C) and thermistors fired at 850°C were analysed by X-ray diffraction (XRD) analysis with a Philips PW 1710 X-ray diffractometer using Cu K_α radiation. X-ray spectra were measured from 2 Θ=20° to 2 Θ=70° in steps of 0.02°.

Cold (from -25°C to 25°C) and hot (from 25°C to 125°C) TCRs were calculated from resistivity measurements at - 25°C, 25°C, and 125°C. The current noise was measured in dB on 100-mW loaded resistors using the Quan Tech method (Quan Tech Model 315-C).

Results and discussion

2041 resistors

X-ray spectra of dried 2041 resistors and resistors fired at 850°C on alumina and LTCC substrates are shown in Fig. 4. The spectra of RuO_2 (denoted RuO2) and $Pb_2Ru_2O_{6.5}$ (denoted RU) are added. As mentioned above the conductive phase of the 2041 resistor material is based on a mixture of ruthenium oxide and ruthenate. The spectra of 2041 resistors, fired on alumina and LTCC substrates, are nearly the same, which indicates the compatibility of the 2041 with LTCC.

The microstructure of the surface of the 2041 resistor, fired at 850°C is shown in Fig. 5. Cross-sections of the 2041 fired at 850°C on alumina and LTCC substrates are shown in Figs. 6.a and 6.b, respectively. The substrate is on the right. The 2041 resistor is a multiphase mixture consisting of conductive phase (white grains), dark-grey grains (rich in Si and Zr, presumably $SrZrO_4$), and a light-grey glass phase.

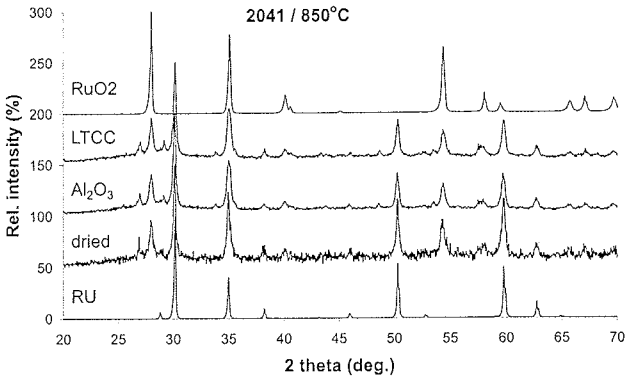

Fig. 4: X-ray spectra of dried 2041 resistors and resistors fired at 850°C on alumina and LTCC substrates. The added spectra of RuO_2 and $Pb_2Ru_2O_{6.5}$ are denoted RuO2 and RU, respectively.

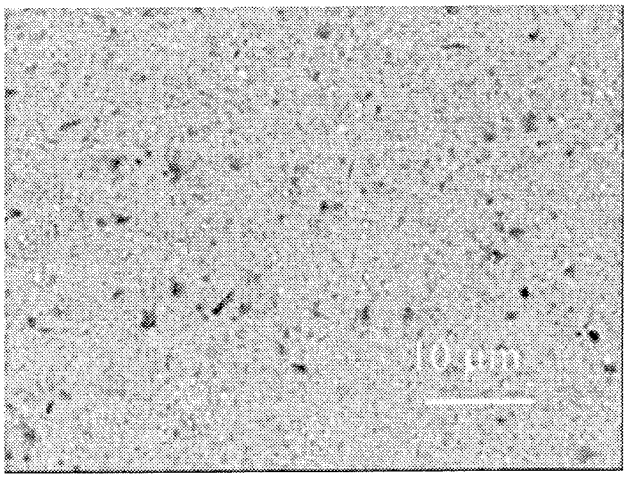

Fig. 5: The microstructure of the surface of the 2041 resistor, fired at 850°C

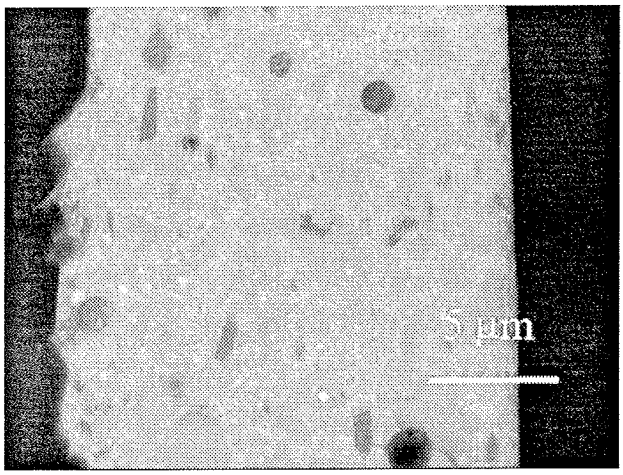

Fig. 6.a: Cross-section of the 2041 resistor, fired at 850°C on alumina. The alumina substrate is on the right.

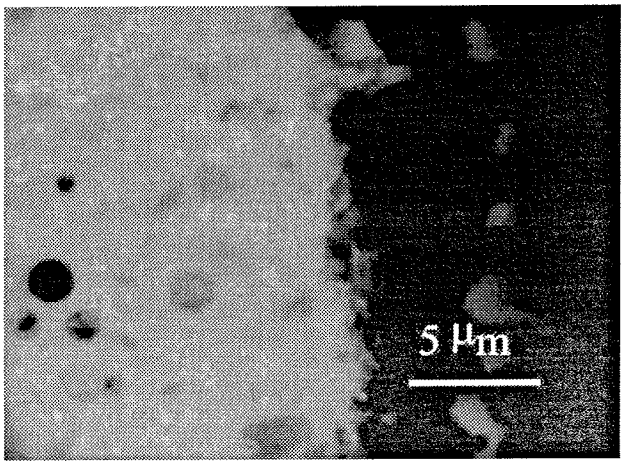

Fig. 6.b: Cross-section of the 2041 resistor, fired at 850°C on LTCC. The LTCC substrate is on the right.

The EDS micro-analyses over the whole cross-sections of the 2041 films (area 15x15 um^2) on the alumina and LTCC substrates are presented in Table 1. The compositions are given for elements and for oxides in at. % and mol. %, respectively. The concentration of oxygen is calculated by difference and not measured directly. The concentrations of the elements are similar for the resistors fired on alumina and on LTCC substrates. This indicates that there was no significant (or observable) interaction between the glassy LTCC material and the 2041 resistor.

Table 1: The EDS analyses of the concentration of elements (in atomic %) and oxides (in mol. %) in the 2041 films fired at 850°C on the alumina and LTCC substrates

Element (at. %)	Al_2O_3 substrate	LTCC substrate	Oxide (mol. %)	Al_2O_3 substrate	LTCC substrate
Mg	/	<1	MgO	/	<3
Al	4	3	$AlO_{1.5}$	11	8
Si	17	17	SiO_2	45	44
Ca	2	4	CaO	5	10
Zn	1	1	ZnO	3	3
Zr	<1	<1	ZrO_2	<3	<3
Ru	6	6	RuO_2	16	15
Ba	1	1	BaO	3	3
Pb	6	5	PbO	16	13
O	67	66			

The electrical characteristics, i.e., sheet resistivities, cold (-25°C to 25°C) and hot (25°C to 125°C) TCRs and noise indices of the 2041 resistors fired on alumina and LTCC substrates are shown in Table. 2. Note that the noise indices are expressed in "dB" and "uV/V". These two units are "connected" with a simple equation, i.e,. noise (dB) = 20 x log noise (uV/V) The dependence of the relative sheet resistivities vs. temperature of the 2041 resistors fired at 850°C on alumina or LTCC substrates is shown in Fig. 7.

Table 2: Sheet resistivities, cold (-25°C to 25°C) and hot (25°C to 125°C) TCRs, and noise indices of the 2041 resistors on alumina and on LTCC substrates.

Substrate	R sheet (ohm/sq.)	Cold TCR ($x10^{-6}$/K)	Hot TCR ($x10^{-6}$/K)	Noise (dB)	Noise (uV/V)
A_2O_3	850	2540	2580	-11	0,28
LTCC	180	3070	3075	-32	0,02

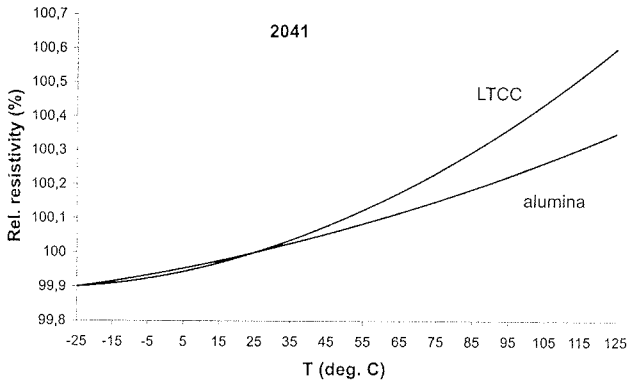

Fig. 7: Relative resistivity vs. temperature of the 2041 resistors fired at 850°C on alumina or LTCC substrates

The electrical characteristics, summarised in the Table 2, tentatively confirm that there is no significant interaction between the 2041 resistor material and the glassy LTCC substrates. The resistivity vs. temperature curve of resistors fired on LTCC substrates is a little more "steep", but the TCR values are still well inside the required +/- 100x10^{-6}/K values. All the presented results, i.e., XRD and EDS analyses as well as electrical characteristics strongly indicate the (very useful) compatibility between the 2041 resistors and the LTCC substrates when resistors are cofired on the LTCC.

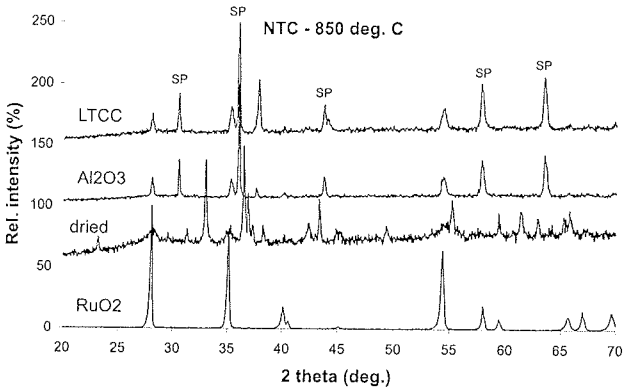

Fig. 8: The X-ray diffraction spectra of the NTC 4993 thermistors fired at 850°C on alumina and on LTCC substrates. The spectrum of ruthenate, denoted "RuO2", is also included. Peaks of spinel phase are denoted "SP".

NTC 4993 thermistors

The X-ray diffraction spectra of the NTC 4993 thermistors dried at 150°C and fired at 850°C on alumina and cofired on LTCC substrates are shown in Fig. 8. The spectrum of ruthenium oxide, denoted "RuO2", is also included in the graph. It is interesting to note that peaks of spinel phase (denoted "SP") appear after firing, but are not present in the dried thick-film. This means that the active phase is formed during the firing and is not included as a prereacted compound. In the fired layers the X-ray analyses show mainly spinel and RuO_2, which is added to the thick-film NTC materials, as mentioned in the Introduction, to decrease the specific resistance and to improve the stability and the current noise. The presence of a few (unmarked) X-ray peaks, most notably the one at 2 Θ = 38°, could be tentatively attributed to un-reacted oxides. The temperature of the formation of the spinel solid solution in the investigated thick-film NTC thermistors, as seen from the X-ray spectra, is relatively low. In the production of discrete components the required firing temperatures are from 1000°C to over 1200°C /11,14,24,25/. The lower temperature of the spinel synthesis in thick-film materials as compared to bulk ceramics is presumably due to the presence of the liquid glass phase which appears in thick-film resistors at temperatures around 700°C /26,27/.

The microstructure of the surface of the NTC 4993 thermistors fired at 850°C is shown in Fig. 9. The microstructure is glassy and porous with pore dimensions up to 10

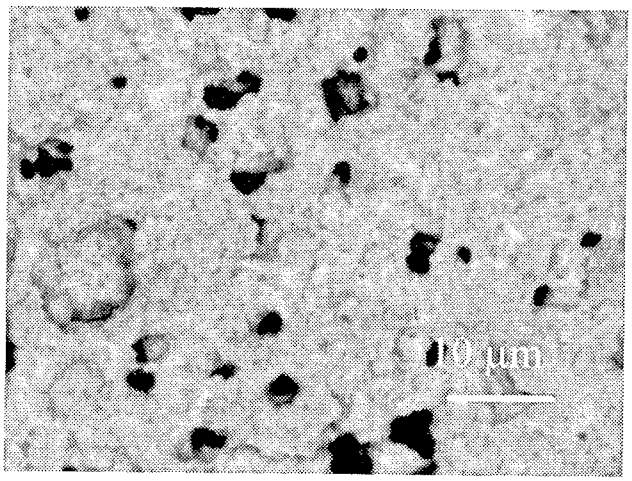

Fig. 9: The microstructure of the surface of the NTC 4993 thermistor, fired at 850°C

um. The lighter phase is a glass phase. Cross-sections of the NTC 4993 thermistors fired at 850°C on alumina and LTCC substrates are shown in Figs. 10.a and 10.b. respectively. In both cases the films are porous. The interaction layer on the interface between the NTC films and the substrates is observed for both substrates. The thin, light-coloured phase on the alumina side is lead-oxide rich and indicates the diffusion of PbO into the alumina ceramics. The darker interface within the LTCC substrate near the interface is rich in alumina which presumably diffused from the LTCC into the NTC film.

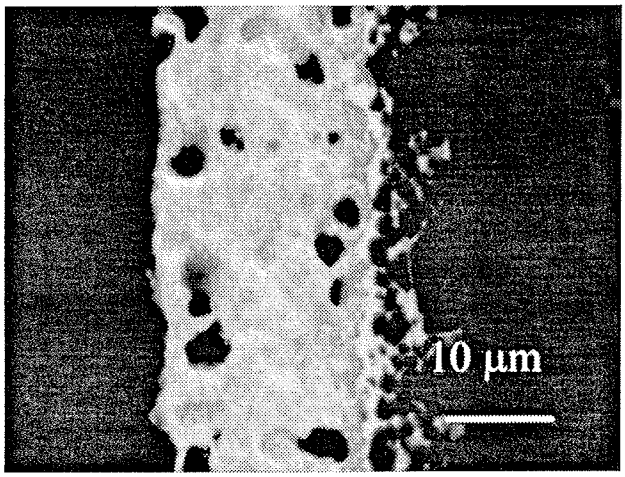

Fig. 10.a: Cross-section of the 4993 NTC thermistor, fired at 850°C on alumina. The alumina substrate is on the right

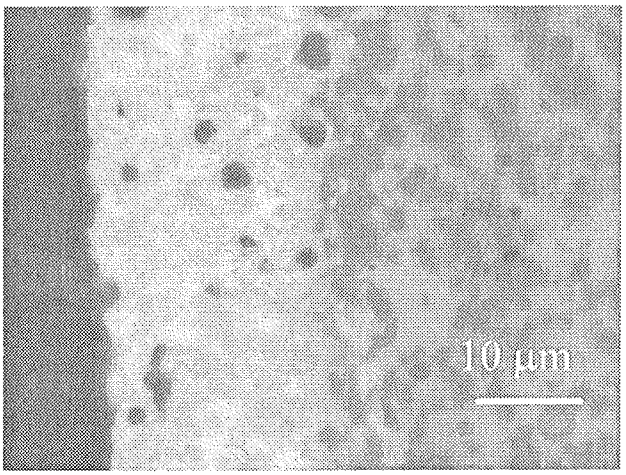

Fig. 10.b: Cross-section of the 4993 NTC thermistor, fired at 850°C on LTCC. The LTCC substrate is on the right

The overall analyses of the NTC layers (area 15x15 um^2) showed the presence of mainly Al, Si, Mn, Co, Ni, Cu, Ru and Pb. As mentioned in the Introduction, copper oxide and ruthenium oxide are added to lower the specific resistance of Mn-Co-Ni solid solutions. The results of the analysis are present in Table 3. The compositions are given for elements and for oxides in at. % and mol. %, respectively. The concentration of oxygen is calculated by difference and not measured directly. The elemental ratio between Mn-, Co- and Ni-oxides is roughly 5/2/1, which puts this composition in the region of solid solutions with the lowest specific resistances between 0.5 and 1 kohm.cm /13/. Note that a higher concentration of SiO_2 in the NTC films fired on LTCC substrates than the films on alumina substrates, indicates a significant diffusion of silica from the LTCC into the thick-film NTC thermistors during firing.

Table 3: The EDS analyses of the concentration of elements (in atomic %) and oxides (in mol. %) in the NTC 4993 thermistors fired at 850°C on the alumina and LTCC substrates

Element (at. %)	Al_2O_3 substrate	LTCC substrate	Oxide (mol. %)	Al_2O_3 substrate	LTCC substrate
Al	7	7	$AlO_{1.5}$	17	15
Si	5	9	SiO_2	12	19
K	<1	<1	$KO_{0.5}$	<2	<2
Ca	<1	<1	CaO	<2	<2
Mn	10	11	MnO_x	24	23
Co	4	4	CoO_x	10	9
Ni	2	2	NiO	5	4
Cu	6	6	CuO	14	13
Ru	2	2	RuO_2	5	4
Pb	4	4	PbO	10	9
O	57	55			

The electrical characteristics, i.e., sheet resistivities, cold (-25°C to 25°C) and hot (25°C to 125°C) TCRs, beta factors and noise indices of the NTC 4994 thermistors fired on alumina and LTCC substrates are shown in Table. 4. Note that the noise indices are expressed in "dB" and "uV/V". The noise indices are expressed in "dB" and "uV/V".

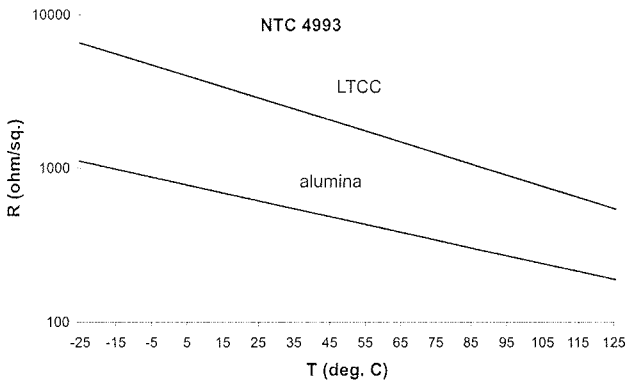

Fig. 11: Logarithm of sheet resistivities vs. temperature of NTC 4994 thermistors fired at 850°C on alumina or LTCC substrates.

Table 4: Sheet resistivities, cold (-25°C to 25°C) and hot (25°C to 125°C) TCRs, beta factors and noise indices of the 2041 resistors on alumina and on LTCC substrates.

Substrate	R sheet (ohm/sq.)	Cold TCR ($x10^{-6}$/K)	Hot TCR ($x10^{-6}$/K)	B (K)	Noise (dB)	Noise (uV/V)
Al_2O_3	550	-22700	-6510	1240	-12.2	0.25
LTCC	2250	-41500	-7550	1660	7.4	2.34

These two units are "connected" with a simple equation - see the comments relating to Table 2. The dependence of the relative sheet resistivities vs. temperature of the 2041 resistors fired at 850°C on alumina or LTCC substrates is shown in Fig. 11.

The sheet resistivities of the NTC 4993 thick-film thermistors (nominal sheet resistivity 1 kohm/sq,) are, at room temperature, around 500 ohm/sq. on alumina, while on the LTCC substrates they are four times higher. Similarly, the cold and hot TCRs and the beta factors of the thermistors fired on LTCC are higher than the values fired on alumina. These results could be attributed to the diffusion of the glassy phase, mainly SiO_2, from the LTCC substrates into the NTC films during firing. The additional glass presumably "breaks up" some of the conductive paths through the resistor film, thereby increasing the sheet resistivities as well as the noise indices. However, if the higher current noise of the NTC 4993 thermistors fired on LTCC substrates is acceptable the investigated thick-film NTC materials could be used on LTCC substrates.

Conclusions

Low-Temperature Co-fired Ceramic (LTCC) materials, which are sintered at the low temperatures typically used for thick-film processing, i.e. around 850°C, are convenient and widespread technique for MCM-C (Ceramic multi-chip modules). LTCC materials are based either on crystallizable glass or a mixture of glass and ceramics. As most of the thick-film resistors were developed for firing on alumina substrates their compatibility with (rather glassy) LTCC substrates needed to be evaluated. The "normal", i e., low TCR thick-film resistor 2041 (10 kohm/sq., Du Pont) and the 4993 NTC thermistor (1 kohm/sq., EMCA Remex) were fired on 96% alumina and co-fired on green Du Pont LTCC 951 tapes. The electrical and microstructural characteristics were compared.

The X-ray spectra of the 2041 resistors fired on alumina and LTCC substrates are nearly the same, which indicates the compatibility of the 2041 with LTCC. Also, the electrical characteristics of 2041 resistors fired on both substrates are similar indicating that the resistors are compatible with the LTCC material. The EDS analyses did not show any significant interaction between the 2041 resistors and the LTCC substrates.

For the NTC 4993 thermistors the XRD analysis showed that the spinel active phase is formed during the firing and is not included as a pre-reacted compound. There were no significant differences in the X-ray spectra between thermistor films fired on alumina or on LTCC substrates. The electrical characteristics, i.e., the sheet resistivities, beta factors and noise indices of the thermistors fired on LTCC substrates as compared to films fired on alumina significantly increased, indicating the interaction between the thermistor layers and the LTCC substrates. The changes in the electrical parameters were attributed to the diffusion of a silica-rich phase from the LTCC substrates into the thermistor films.

Acknowledgements

The authors wish to thank Mr. Mitja Jerlah (HIPOT-HYB) for printing and firing the samples as well as for measuring the electrical characteristics. The financial support of the Slovenian Research Agency is gratefully acknowledged.

References

/1./ A. A. Shapiro, D. F. Elwell, P. Imamura, M. L. MeCartney, Structure-property relationships in low-temperature cofired ceramic, Proc. 1994 Int. Symp. on Microelectronics ISHM-94, Boston, 1994, 306-311

/2./ J.-H. Jean, C.-R. Chang, Camber development during cofiring Ag-based low-dielectric-constant ceramic package, J. Mater. Res., 12, (10), (1997), 2743-2750

/3./ R. E. Doty, J. J. Vajo, A study of field-assisted silver migration in low temperature cofirable ceramic, Proc. 1995 Int. Symp. on Microelectronics ISHM-95, Los Angeles, 1995, 468-474

/4./ R. E. Doty, J. J. Vajo, A study of field-assisted silver migration in low temperature cofirable ceramic, Proc. 1995 Int. Symp. on Microelectronics ISHM-95, Los Angeles, 1995, 468-474

/5./C.-J. Ting, C.-S. Hsi, H.-J. Lu, Interactions between ruthenium-based resistors and cordierite-glass substrates in low temperature co-fired ceramics, J. Am. Ceram. Soc., 83, (12), (2000), 23945-2953

/6./ W. K. Jones, Y. Liu, B. Larsen, P. Wang, M. Zampino, Chemical, structural and mechanical properties of the LTCC tapes, Proc. 2000 Int. Symp. on Microelectronics IMAPS-2000, Boston, 2002, 669-674

/7./ M. A. Rodrigues, P. Yang, P. Kotula, D. Dimos, Microstructure and phase development of buried resistors in low temperature co-fired ceramics, J. Electroceramics, 5, (3), (2000), 217-223

/8./ A. Dziedzic, L. J. Golonka, J. Kita, H. Thust, K-H. Drue, R. Bauer, L. Rebenklau, K-J. Wolter, Electrical and stability properties and ultrasonic microscope characterization of low temperature

co-fired ceramics resistors, Microelectronics Reliability, 41, (2001), 669-676

/9./ P. Yang, M. A. Rodrigues, P. Kotula, B. K. Miera, D. Dimos, Processing, microstructure, and electric properties of buried resistors in low-temperature co-fired ceramics, J. Appl. Phys., 89, (7), (2001), 4175-4182

/10./ C-S. His, D-F. Chen, F-M. Shieh, S-L. Fu, Processing of LTCC with embedded RuO_2-based resistors, Mater. Chem. Phys., 78, (2002), 67-72

/11./ J. L. Martin de Vidales, P. Garcia-Chain, R. M. Rojas, E- Vila, O. Garcia-Martinez, Preparation and characterisation of spinel-type Mn-Ni-Co-O negative temperature coefficient ceramic thermistors, J. Mater. Sci., 33, (6), (1998), 1491-1496

/12./J. Huang, Y. Hao, H. Lin, D. Zhang, J. Song, D. Zhou, Preparation and characteristics of the thermistor materials in the thick-film integrated temperature-humidity sensor, Mater. Sci. Eng., B99, (1-3), (2003), 523-526

/13./ M. Prudenziati (Ed.), Thick Film Sensors, Elsevier, Amsterdam, 1994, 127-150

/14./ M. L. Martinez Sarrion, M. Morales, Preparation and characterization of NTC thermistors based on $Fe_{2+y}Mn_{1-x-y}Ni_xO_4$, J. Mater. Sci., 30, (10), (1995), 2610-2613

/15./ K. Park, D. J. Bang, Electrical properties of Ni-Mn-Co-(Fe) oxide thick-film NTC thermistors prepared by screen printing, J. Mater. Sci.: Materials in Electronics, 14, (2003), 81-87

/16./ D. Metz, P. Caffin, R. Legros, A. Rousset, The preparation, characterization and electrical properties of copper manganite spinels, $Cu_xMn_{3-x}O_4$, 0<x<1, J. Mater. Sci., 24, (1), (1989), 83-87

/17./ R. Metz, Electrical properties of NTC thermistors made of manganite ceramics of general spinel structure: $Mn_{3-x-y}M_xN_yO_4$ 0<x+y<1; M and N being Ni, Co or Cu. Aging phenomenon study, J. Mater. Sci., 35, (18), (200), 4705-4711

/18./ P. R. van Loan, Conductive ternary oxides of ruthenium, and their use in thick film resistor glazes, Ceram. Bull., 51, (3), (1972), 231-233, 242

/19./ J. W. Pierce, D. W. Kuty, J. R. Larry, The chemistry and stability of ruthenium based resistors, Solid State Technol., 25, (10), (1982), 85-93

/20./ Y. D. Hao, L. J. Chen, H. Lin, D. X. Zhou, S. P. Gong, Research on NTC thermally sensitive powder materials for thick-film thermistors, Sensors and Actuators, A35, (3), (1993), 269-272

/21./ M. Hrovat, J. Holc, S. Drnovšek, D. Belavič, J. Bernard, M. Kosec, L. Golonka, A. Dziedzic, J. Kita, Characterization of PZT thick films fired on LTCC substrates. J. Mater. Sci. Lett., 22, (2003), 1193-1195

/22./ M. Hrovat, D. Belavič, Z. Samardžija, J. Holc, A characterisation of thick film resistors for strain gauge applications, J. Mater. Sci., 36, (11), (2001), 2679-2689

/23./ D. Belavič, M. Hrovat, M. Pavlin, M. Santo Zarnik, Thick-film technology for sensor applications, Informacije MIDEM, 33, (1), (2003), 45-48

/24./ E. D. Macklen (Ed.), Thermistors, Electrochemical Publications Ltd., Ayr, 1979, 16-28

/25./ K. Park, Improvement in electrical stability by addition of SiO_2 in $(Mn_{1.2}Ni_{0.78}Co_{0.87-x}Cu_{0.15}Si_x)O_4$ negative temperature coefficient thermistors, Scripta Materialia, 50, (2004), 551-554

/26./ M. Hrovat, F. Jan, An investigation of thick film resistor materials properties during firing process, Hybrid circuits, 14, (1987), 25-29

/27./ M. Hrovat. A. Benčan, D. Belavič, J. Holc, G. Dražič, The influence of firing temperatures on the electrical and microstructural characteristics of thick film resistors for strain gauge applications, Sensors and Actuators, A103, (2003), 341.352

Marko Hrovat, Janez Holc, Jena Cilenšek
Jožef Stefan Institute, Jamova 39,
SI-1000 Ljubljana, Slovenia
Phone: +386 1 477 3900,
e-mail: marko.hrovat@ijs.si

Darko Belavič,
HIPOT-R&D, d.o.o., Trubarjeva 7,
SI-8310 Sentjernej, Slovenia

Jaroslaw Kita, Leszek Golonka, Andrzej Dziedzic
Wroclaw University of Technology, Wybrzeze
Wyspianskiego 27, 50-370 Wroclaw, Poland

Prispelo (Arrived): 03.06.2005 *Sprejeto (Accepted): 30.09.2005*